Internal Vaporization in Porous Materials Under Laser Irradiation

D. E. Hastings* and A. A. Rigos†
Physical Sciences, Inc., Andover, Massachusetts

Under laser irradiation, a porous material may vaporize within its pores as well as at the surface. The effect of this phenomenon is examined for pores with a high degree of connectivity and for a pore tree model. It is shown that in the former case, the internal vaporization of material is bounded by the rate at which vapor can escape from inside the porous substance. This rate is sufficiently large so that significant modification of the internal temperature profile may result. For the pore tree model, the buildup of vapor pressure in the pores suppresses the internal vaporization. An upper bound on the mass flow rate from the pore tree is derived when the back pressure is self-consistently included. For pore trees of interest, this bound is small enough so that significant modification of the internal temperature profile will not result; however, material damage may occur due to the high internal pressures.

I. Introduction

MOST materials under high-power laser irradiation undergo surface vaporization and recession.[1-3] When the laser energy is absorbed in-depth in the material, numerical simulations have shown that the internal temperature of the material can exceed the surface temperature. As energy is used at the surface for vaporization and recession, the surface temperature tends to stay close to the equilibrium vaporization temperature of the material at 1 atm. Inside a nonporous solid material, internal vaporization does not occur and the internal temperature can rise above the $p = 1$ atm vaporization temperature. However, if the material is porous (i.e., has internal voids), vaporization may occur inside the pores. This internal process has been largely ignored in studies of laser heating of materials. One would expect that the loss of energy associated with the vaporization process would keep the internal temperature from rising. If this happens, the temperature profile may be substantially different from what one obtains with no internal vaporization. Internal vaporization also may cause discrete mass removal from the material. This can occur if the pressure in the pores builds up until it exceeds the fracture stress of the material. It should be noted that internal vaporization can occur in materials which are not initially porous but have a component that can pyrolyze. After the pyrolysis is complete, a porous char is left that can then undergo vaporization.

In this paper, we study the problem of the effect of internal vaporization on the internal pressure in a porous material under laser irradiation. Section II is an introduction to pore structure theory. In Sec. III, we consider a porous material with a high degree of connectivity. This means that the vaporizing material can escape from the pores before any pressure buildup occurs. We show that the internal vaporization is bounded by the rate at which vapor can escape from the front surface. In Sec. IV–VI, we address the opposite limit, where the pressure builds up in the pores because of the high internal surface area and low exit area. The pressure buildup suppresses the internal vaporization. An upper bound on the rate at which vapor can escape is obtained for this case. In Sec. VII, we discuss future directions for this research.

Received March 23, 1987; revision received Sept. 23, 1987.

*Consultant; currently Associate Professor, Department of Aeronautics and Astronautics, Massachusetts Institute of Technology.
†Principal Scientist; currently Assistant Professor, Department of Chemistry, Merrimack College.

II. Pore Structure Theory

The effect of pores on a material may be characterized by two quantities. The first is the internal surface area of the pores per unit mass of solid material (S_p). If the material has a volume V and bulk density ρ, then for cylindrical pores, S_p is defined by

$$S_p = \sum_{\text{all pores}} \frac{2\pi}{\rho V} \int r_p \mathrm{d}l_p \tag{1}$$

where r_p is the pore radius and l_p is the pore length. This quantity can be measured for a given material by using N_2 or CO_2 Brunaner, Emmett, and Teller (BET)[4] adsorption isotherm method. The other measure is the porosity θ which is the fractional volume in the pores defined by

$$\theta = \sum_{\text{all pores}} \frac{\pi}{V} \int r_p^2 \mathrm{d}l_p \tag{2}$$

If most of the surface area of the pores is in the smallest pores,[5] we can use a $1/r_p^3$ pore distribution function to approximate the integrals in Eqs. (1) and (2) and obtain

$$S_{p_i} \simeq 2\,\theta_i / r_{p_{\min}}\,\rho \tag{3}$$

where $r_{p_{\min}}$ is the minimum pore radius and subscript i denotes initial values.

The mass vaporization rate $\dot{m}_v(T,p)$ is taken to be given by the emission of a half-Maxwellian distribution of vapor from a surface into a flow of the vapor that provides a finite back pressure on the surface. This problem has been investigated in Ref. 3, where it is shown that $\dot{m}_v$ can be written as

$$\dot{m}_v(T,p) = \dot{m}_{v_o}(T) g(p/p_s) \tag{4}$$

where $\dot{m}_{v_o}(T)$ is the mass flow rate for emission from a surface into a vacuum

$$\dot{m}_{v_o}(T) = p_s / R_G T\,(R_G T/2\pi)^{1/2} \tag{5}$$

R_G is the gas constant for the vapor, and p_s is the equilibrium vapor pressure given by the Clausius-Clapeyron relation

$$p_s = p_o \exp\left[\frac{\Delta H_V}{R_G}\left(\frac{1}{T_o} - \frac{1}{T}\right)\right] \tag{6}$$

In Eq. (6), ΔH_v is the heat of vaporization and T_o is the temperature at which the vapor pressure is p_o. This is typically

chosen to be the vaporization temperature when $p_o = 1$ atm. In Eq. (4), the function $g(p/p_s)$ is a measure of the reduction of the vaporization rate as a result of a finite back pressure in the pores. Given this, $g(p/p_s)$ must have the following properties:

$$g = 1 \text{ for } p = 0 \tag{7}$$

$$g = 0 \text{ for } p = p_s \tag{8}$$

Equation (7) states that if there is no pressure buildup in the pores then the mass flow rate, $\dot{m}_v(T,p)$, is the vacuum emission rate $\dot{m}_{v_o}(T)$. This would be the case if the pressure in the pores is relieved very quickly; for example, if all the pores were highly connected. Equation (8) states that when the pressure in the pores p builds up to the saturation pressure p_s then the system is at equilibrium and as much mass condenses on the surface as leaves it; hence, no net vaporization is possible. This would be expected to happen when the pore structure resists fluid flow and results in a vapor pressure buildup. In this section and the following section we shall explore these two limits.

III. Internal Vaporization in a Material with Highly Connected Pores (Sand Model)

In the limit where the internal pore structure is highly connected and the pressure does not build up in the pores to suppress the vaporization, the internal vaporization is still limited by the rate at which mass can escape from the front surface of the material. We can obtain this as follows: by conservation of mass we must have at the front face

$$\dot{M}_{\text{pores}} = \dot{m}_{\text{pores}} A^f_{\text{pores}} \tag{9}$$

where A^f_{pores} is the frontal area of the pores and $\dot{M}_{\text{pores}}$ is the total mass flow rate out of the pores, whereas $\dot{m}_{\text{pores}}$ is the mass flow rate per unit area out of the pores. The total mass flow rate from the front surface is

$$\dot{M}_{\text{total}} = \dot{m}_{\text{solid}} A_{\text{solid}} + \dot{m}_{\text{pores}} A^f_{\text{pores}} \tag{10}$$

where A_{solid} is the solid surface area, and $\dot{m}_{\text{solid}}$ is the mass flow rate per unit area from the solid area. If the emission is taking place into a vacuum, then $\dot{m}_{\text{solid}}$ is given by well-known formula $\dot{m}_{\text{solid}} = mn\bar{c}/4 = \dot{m}_{v_o}$, where the mean velocity $\bar{c}$ is given by

$$\bar{c} = 4\,(R_G T/2\pi)^{1/2}$$

The mass flow from the pores is bounded when the flow chokes at the exit. So $\dot{m}_{\text{pores}} \leq \rho^* u^*$, where the ρ^* denotes the density at the speed of sound $u^* = \sqrt{\gamma R_G T}$. If we multiply and divide the RHS by $\dot{m}_{v_o} = \rho\,(R_G T/2\pi)^{1/2}$, we obtain

$$\dot{m}_{\text{pores}}\,(\rho^*/\rho)\,\sqrt{2\pi\gamma}\,\dot{m}_{v_o}$$

If we take the flow in the pore as isentropic, then we can write

$$\frac{\rho}{\rho^*} = \left[1 - \frac{\gamma - 1}{\gamma + 1}\right]^{\frac{1}{\gamma - 1}}$$

such that

$$\dot{m}_{\text{pores}} = \dot{m}^{\text{sand}}_{\text{pores}} \leq (2\pi\gamma)^{1/2}\,[2/(\gamma + 1)]^{1/(\gamma - 1)}\,\dot{m}_{v_o} \tag{11}$$

From Eq. (11) and for $\gamma = 1.28$, we obtain

$$\dot{m}^{\text{sand}}_{\text{pores}} \simeq 1.8\,\dot{m}_{v_o} \tag{12}$$

We see that the internal vaporization can increase the total mass loss up to a factor of 1.8 ($A_{\text{solid}} \ll A^f_{\text{pores}}$ and $\gamma = 1.28$). This means that the energy lost in vaporization increases and the internal temperature must decrease. This represents an upper bound on the effect of internal vaporization and may lead to significant changes in the temperature profile.

IV. Internal Vaporization in a Pore Tree: General Formulation

The pore structure is important in determining the controlling processes in the production of vapor inside the pores. The opposite limit of the limit considered in Sec. II is where the pressure builds up in the pores and suppresses the vaporization. We shall consider this process within the context of the pore tree model developed in Refs. 5 and 6. The unique feature of this model is that it possesses cylindrical pores whose branching sequence is depicted as an ordinary tree or river system. For our purposes, the primary significance of the pore tree is the influence of the pore branching sequence. Most of the surface area of the pore tree is contained in the fine pores; therefore, most of the vapor production takes place in the fine pores. However, for the vapor to escape, it must diffuse through the branches and escape at the base of the tree trunk. This allows the back pressure to build up and suppress the vaporization.

The pore tree is shown in Fig. 1 and is characterized by a trunk length l_t, a trunk radius r_t, a minimum pore radius $r_{p_{\min}}$ and a maximum pore radius $r_{p_{\max}}$. The number of branches of radius r_p is given by

$$N = r_t^2/r_p^2 \tag{13}$$

which corresponds to a pore distribution function proportional to $1/r_p^3$.[5] This indicates that when $r_p = r_t$ there is only one branch (the trunk) and that as r_p decreases the number of branches increases. The metric factor, or relationship between skewed length along the tree to radius, is

$$\frac{\mathrm{d}r_p}{\mathrm{d}y} = \frac{r_p}{l_t} \tag{14}$$

which implies that the total skewed length of the tree is $l_t \ell n(1/\lambda)$, where $\lambda^{-1} = r_{p_{\max}}/r_{p_{\min}}$. We chose $r_{p_{\max}} = r_t$ so that $\lambda = r_{p_{\min}}/r_t$. The surface area S_a is

$$S_a = \sum_K \int 2\pi r_p\, N \mathrm{d}y = \sum_K (2\pi l_t r_t^2/r_{p_{\min}})(1 - \lambda) \tag{15}$$

where K is the number of pore trees. This supports the contention that most of the surface area is in the smallest pores. The porosity of volume V is

$$\theta = (1/V) \sum_K \int \pi r_p^2 \mathrm{d}y = (1/V) \sum_K \pi l_t r_t^2 \ell n(1/\lambda) \tag{16}$$

Within the pore tree, the flow speed $\bar{u}$ will depend on the pore size.[7] If the pores are very small then the flow velocity will be

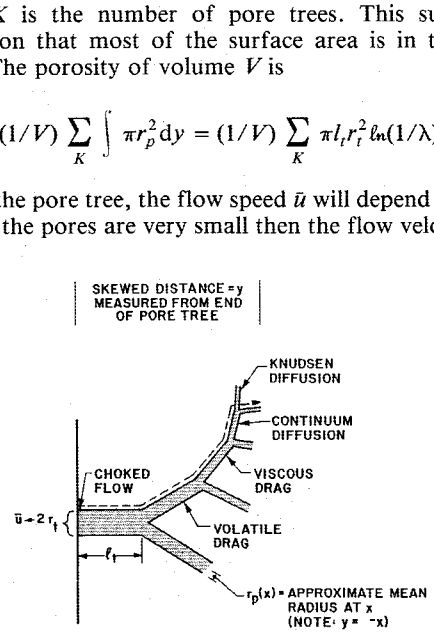

Fig. 1 Pore tree model.

determined by diffusion of the vapor, with the step size for diffusion determined by the pore radius. This is Knudsen diffusion and gives $\bar{u} = D_{\mathrm{Kn}}\, \mathrm{d}(\ell n p_G)/\mathrm{d}y$, where p_G is the gas pressure and D_{Kn} = Knudsen diffusion coefficient[8] = $2/3\, r_p(2T/m)^{1/2}$. The next regime for $\bar{u}$ is where gas phase collisions dominate the transport process.[9] We have $\bar{u} = -D_c\, \mathrm{d}(\ell n p_G)/\mathrm{d}y$, where $D_c = 4/3\ \mu_G(T)\rho_G$ and $\mu_G(T)$ is gas viscosity and ρ_G the gas density. As the velocity increases, it next becomes limited by viscous drag, giving $\bar{u} = -\{r_p^2/[8\mu_G(T)]\}\mathrm{d}p_g/\mathrm{d}y$. This eventually gives way to volatile drag, where $\bar{u} = -\{r_p/[2\dot{m}_v(T,p_G)]\}\mathrm{d}p_G/\mathrm{d}y$ and is determined by the introduction of slow moving vapor into the flow. Finally, if the exit pressure from the tree is low enough the flow will choke, so that $\bar{u} = \sqrt{\gamma R_G T}$, where γ = ratio of specific heats. This is expected in the trunk of the tree.

The specification of $\bar{u}$ represents a solution of the momentum balance equation. To obtain the self-consistent pressure in the tree, we need the continuity and energy balance equations. For this study, we shall assume that the temperature is constant over the region of interest, so that the energy balance equation drops out. This leaves the continuity equation, which is

$$\frac{\mathrm{d}}{\mathrm{d}y}(N\rho_G \pi r_p^2 \bar{u}) = N\dot{m}_v(T,p)\ 2\pi r_p \tag{17}$$

This equation balances the mass flow rate out of a pore with the mass generation rate. The boundary conditions are

$$\bar{u} = 0 \qquad \text{at } r = r_{p_{\min}} \tag{18}$$

$$\bar{u} = \sqrt{\gamma R_G T} \quad \text{at } r = r_t \simeq r_{p_{\max}} \tag{19}$$

The flow regime at any given r_p will be determined by which effect dominates the momentum balance. We are interested in materials where $r_{p_{\min}} \gtrsim 0.1\ \mu$m and for such pore sizes it is easy to show that the flow will be either in the viscous or volatile regime.

V. Flow in a Pore Tree—Volatile Regime

If the flow is entirely in the volatile regime, then it is possible to solve the continuity equation exactly. From Eqs. (14), (15) and (17), and using

$$\bar{u} = \frac{-r_p}{2\dot{m}_{v_o} g(p_G/p_s)} \frac{\mathrm{d}p_G}{\mathrm{d}y} \tag{20}$$

we obtain the continuity equation as

$$-r_p^2 \frac{\mathrm{d}}{\mathrm{d}r_p}\left[\frac{p_G}{g(p_G/p_s)} r_p^2 \frac{\mathrm{d}p_G}{\mathrm{d}r_p}\right] = 4l_t^2 R_G T_G \dot{m}_{v_o}^2 g(p_G/p_s) \tag{21}$$

subject to the boundary conditions of Eq. (18) and (19). If we define $x = 1/r_p$, $p_2 = p_G^2/2$, $\bar{p}_2 = p_G^2/p_s^2$, and $\beta^2 = 4l_t^2 R_G T_G \dot{m}_{v_o}^2$, then the continuity equation becomes

$$\frac{1}{g(\bar{p}_2)} \frac{\mathrm{d}}{\mathrm{d}x}\left[\frac{1}{g(\bar{p}_2)} \frac{\mathrm{d}}{\mathrm{d}x} p_2\right] + \beta^2 = 0 \tag{22}$$

subject to

$$\frac{1}{g(\bar{p}_2)} \frac{\mathrm{d}p_2}{\mathrm{d}x} \to 0 \text{ as } x \to \frac{1}{r_{p_{\min}}} \tag{23}$$

$$\frac{1}{g(\bar{p}_2)} \frac{\mathrm{d}p_2}{\mathrm{d}x} = (2p_2\gamma)^{1/2}\beta \text{ as } x \to \frac{1}{r_t} \tag{24}$$

This equation can be solved by defining

$$y(p_2) = x'(p_2) g(\bar{p}_2)$$

where $x' = \mathrm{d}x/\mathrm{d}p_2$. At this point, it is easy to show that a necessary and sufficient condition for choked flow at the pore tree exit is if

$$p_2 = p_{2t} \qquad \text{at } x = 1/r_t \tag{24a}$$

then

$$p_2 = p_{2t}(\gamma+1) \quad \text{at } x = 1/r_{p_{\min}} \tag{24b}$$

This solution for $y(p_2)$ is

$$y(p_2) = [2^{1/2}\beta\ (p_{2t}^{(\gamma+1)} - p_2)^{1/2}]^{-1} \tag{25}$$

This gives an implicit expression for p_2:

$$\frac{r_p}{r_{p_{\min}}} = \left\{1 - \frac{r_{p_{\min}}}{2^{1/2}\beta}[p_{2t}(\gamma+1)]^{1/2} \int_{\bar{p}}^{1} \frac{\mathrm{d}\bar{p}}{g(\bar{p})(1-\bar{p})^{-1/2}}\right\}^{-1} \tag{26}$$

where $\bar{p} = p_2/[p_{2t}(\gamma+1)]$ and $1/(\gamma+1) \le \bar{p} \le 1$ in the tree. From Eq. (26) we can obtain the pressure at the end of the trunk from

$$p_{2t} = \frac{2\beta^2}{r_{p_{\min}}^2(\gamma+1)}\left(1 - \frac{r_{p_{\min}}}{r_t}\right)^2 \left[\int_{1/\gamma+1}^{1} \frac{\mathrm{d}\bar{p}}{g(\bar{p})(1-\bar{p})^{1/2}}\right] \tag{27}$$

and then the pressure in the smallest pore is given from $p_{2t}(\gamma+1)$. Suppose we argue that in the smallest pore we expect that the pressure is close to the saturation vapor pressure ($p_G/p_s \simeq 1$ at $r = r_{p_{\min}}$ or $p_2 = p_s^2/2$ at $x = 1/r_{p_{\min}}$). If this expression for the normalized pressure $p_2 = p_G/p_s$ is substituted into Eq. (24b), it gives a value for p_{2t} equal to $p_s^2/[2(\gamma+1)]$. This means that at the end of the trunk [Eq. (24a)], the pressure ratio is

$$p_G/p_s = 1/\sqrt{\gamma+1} \tag{27a}$$

which is equal to 0.66 for $\gamma = 1.28$. This enables us to put a nontrivial bound on the suppression of the mass flow due to back pressure

$$\dot{m}_v = \dot{m}_{v_o}\, g(p_G/p_s) < \dot{m}_{v_o}\, g(1/\sqrt{\gamma+1}) \tag{28}$$

From Ref. 3, it is possible to evaluate $g(p)$ numerically and obtain $g(1/\sqrt{\gamma+1}) \simeq 0.50$ for $\gamma = 1.28$. Therefore, we can conclude that self-consistent inclusion of the back pressure will reduce the mass flow rate by a minimum of 50% for a $\gamma = 1.28$ vapor.

We can obtain another estimate of the effect of self-consistent back pressure by considering the total mass flow from the end of the tree with and without the self-consistent pressure effect. The total mass vaporized per second is

$$\dot{M} = \int \dot{m}_v\, 2\pi r_p\, N\mathrm{d}y = 2\pi l_t r_t \dot{m}_{v_o} \int_{r_{p_{\min}}}^{r_t} g(p)\frac{\mathrm{d}r_p}{r_p^2} \tag{29}$$

In Eq. (29), the weighting factor $1/r_p^2$ in the integral accounts for the bifurcation of the pore tree into branches as the pore radius decreases. The total mass vaporized per second with no suppression ($\dot{M}_{ns}$) is obtained by setting $g(p) \equiv 1$ to give

$$\dot{M}_{ns} = 2\pi l_t r_t^2 \dot{m}_{v_o}\left(\frac{1}{r_{p_{\min}}} - \frac{1}{r_t}\right) \tag{30}$$

Hence, a measure of the effect of the suppression is $\dot{M}/\dot{M}_{ns}$. From Eqs. (29) and (30), and using the solution for p found previously, we obtain

$$\frac{\dot{M}}{\dot{M}_{ns}} = \frac{1}{2}\left(\frac{\gamma}{\gamma+1}\right)^{1/2}\left[\int_{1/\gamma+1}^{1} \frac{\mathrm{d}\bar{p}}{g(\bar{p})(1-\bar{p})^{1/2}}\right]^{-1} = \sigma(\gamma) \tag{31}$$

This integral can be evaluated numerically for a given γ. For $\gamma = 1.28$, we find $\dot{M}/\dot{M}_{ns} \simeq 0.1$. An interesting conclusion from

Eq. (31) is that the ratio $\dot{M}/\dot{M}_{ns}$ in the volatile regime is independent of the temperature or details of the pore tree ($r_{p_{\min}}$, r_t, l_t). This enables us to say quite generally that for pores in the volatile regime the self-consistent inclusion of back pressure will reduce the total mass flow rate by approximately 90% for a $\gamma = 1.28$ vapor.

The mass flow rate out of the front surface for one pore tree is

$$\dot{m}^{\text{tree}}_{\text{pores}} = \frac{\dot{M}}{\pi r_t^2} = \left\{2\left(\frac{l_t}{r_t}\right)\frac{1}{\lambda}(1-\lambda)\,\sigma(\gamma)\right\}\dot{m}_{v_o} \tag{32}$$

If the pressure in the smallest pores is taken to be approximately the saturated vapor pressure, then from Eq. (27) we obtain an expression for λ which has the solution

$$\lambda = \delta/1+\delta \tag{33}$$

where

$$\delta^2 = \frac{8}{\pi}\left(\frac{l_t}{r_t}\right)\left(\frac{T_G}{T_s}\right)\frac{1}{2}\left(\frac{\gamma}{\gamma+1}\right)^{1/2}\frac{1}{\sigma(\gamma)} \tag{34}$$

Since λ is fixed by l_t/r_t and γ, this indicates that the pore parameters may not be freely chosen, if the whole pore tree is to be in this regime. If there are pores with $r_p < r_{p_{\min}}$ given from Eq. (33), then they will be in the viscous regime, but, since $p_G \simeq p_s$, there will be no mass generation coming from those pores.

For $\gamma = 1.28$, we obtain $\lambda \simeq 3(l_t/r_t)^{1/2}/[1+3(l_t/r_t)^{1/2}]$

$$\dot{m}^{\text{tree}}_{\text{pores}} = 0.07\left(\frac{l_t}{r_t}\right)^{1/2}\dot{m}_{v_o} \tag{35}$$

For a typical value of $l_t/r_t = 10$, we obtain $\dot{m}^{\text{tree}}_{\text{pores}} = 0.22\,\dot{m}_{v_o}$. This is considerably below the bound in the last section ($\dot{m}^{\text{sand}}_{\text{pores}} \simeq 1.8\,\dot{m}_{v_o}$), and occurs because the pressure self-consistently suppresses the mass flow.

VI. Flow in a Pore Tree—Viscous Regime

In order to consider pores in both the viscous and volatile regime, it is necessary to solve the continuity equation numerically.

In order to do this, we introduce the following normalizations and definitions.

$$u = \bar{u}/\sqrt{\gamma R_G T} \tag{36}$$

$$r = r_p/r_{p_{\min}} \tag{37}$$

$$p = p_G/p_s \tag{38}$$

$$Re = \sqrt{R_G T}\, r_{p_{\min}}/(\mu_G/\rho) \tag{39}$$

$$\epsilon = r_{p_{\min}}/l_t \tag{40}$$

Here ρ is the saturated vapor density ($\rho = p_s/R_G T$) and Re is a type of Reynolds number. With these definitions we can write the continuity equation as two first-order nonlinear differential equations

$$\frac{du}{dr} = \frac{u^2}{pf(p,r)} + \frac{2}{\epsilon}\frac{1}{r^2}\frac{g(p)}{p}\frac{1}{\sqrt{2\pi\gamma}} \tag{41}$$

$$\frac{dp}{dr} = -\frac{u}{f(p,r)} \tag{42}$$

where

$$\frac{1}{f(p)} = \frac{1}{f_1(r)} + \frac{1}{f_2(p,r)} \tag{43}$$

and

$$f_1(r) = (8r^3/\gamma^{1/2})\,\epsilon Re \tag{44}$$

$$f_2(r) = \frac{r^2\epsilon}{2}\left(\frac{2\pi}{\gamma}\right)^{1/2}\frac{1}{g(p)} \tag{45}$$

The function f_1 arises from flow in the viscous regime, whereas f_2 arises from flow which is dominated by volatile drag. We have neglected the continuum and Knudsen terms, since for typical values of the controlling parameters, these terms are only important for very small pores (<0.1 μm). The Eqs. (41) and (42) are solved subject to the boundary conditions

$$u = 0 \quad \text{at} \quad r = 1 \tag{46}$$

$$u = 1 \quad \text{at} \quad r = 1/\lambda \tag{47}$$

The coupled Eqs. (41) and (42) were solved by using an initial value code to integrate them from $r = 1$ to $1/\lambda$, and by shooting on the value $u = 1$ at $r = 1/\lambda$. We chose to study a graphitic material with $\Delta H_v = 26$ kJ/g, $T_o = 4100$ K, $\rho = 1.8\ g/\text{cm}^3$ and molecular weight of a C_3 vapor $= 36\ g$/mole. Since the viscosity of carbon vapor at high temperatures is not well known, we chose to model it by using an empirically derived expression for hot air, $\mu_G \simeq 3.6 \times 10^{-7}\, T^{0.69}$ kg/m/s. The ratio of specific heats of the vapor was taken as $\gamma = 1.28$.

Typical results are shown in Figs. 2 and 3. In these figures, we took $r_{p_{\min}} = 2$ μm, $r_{p_{\max}} = r_t = 10$ μm and $l_t = 20$ μm. The temperature of the material was taken to be 4700 K. In Fig. 2, p_G/p_s is plotted vs $\ell n(r)$. The skewed length of the pore tree normalized to the trunk length is $l_t\,\ell n(r_t/r_{p_{\min}})$. Therefore, the normalized length of the trunk is 1 and the normalized length

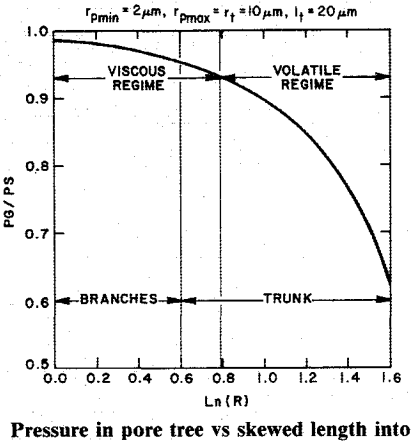

Fig. 2 Pressure in pore tree vs skewed length into tree.

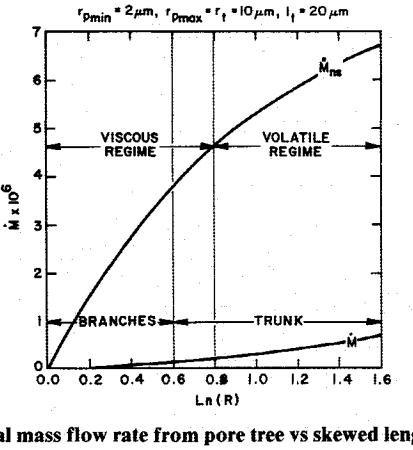

Fig. 3 Total mass flow rate from pore tree vs skewed length into tree.

of the branches is $\ell_n r - 1$. The pressure is seen to fall from the saturation vapor pressure at $r_{p_{\min}}$ to $p_G \simeq p_s/2$ at the exit of the tree. This viscous and volatile regime can be identified from the calculations, and the switch from one to the other occurs for $r_p \simeq 2.22\ r_{p_{\min}} = 4.44\ \mu$m. The pressure ratio between the pressures at the beginning and end of the volatile regime are seen to satisfy Eq. (27a) for $p_s = p_G(r_{p_{\min}})$, such that $p_G(r_{p_{\min}})/p_G(r_t) = \sqrt{(\gamma+1)} = 1.51$. This is what is expected from the analytic solution. We see from Fig. 2 that in the viscous regime the pressure is very close to the saturation vapor pressure. This leads us to expect that most of the contribution to the total mass flow from the tree will come from the volatile regime. This is confirmed in Fig. 3, where the total mass flow $\dot{M}$ is shown against $\ell_n(r)$. We see that 80% of the total mass flow from the end of the tree comes from the volatile regime. This leads us to conclude that for a pore tree structure we can essentially ignore the viscous regime and treat the whole tree as if it were in the volatile regime. In other words, the pore tree with self-consistent pressure suppression acts as if the smallest pores are just cut off and only the larger pores contribute to the vaporization. This is not true if the self-consistent pressure is ignored, as is seen from $\dot{M}_{ns}$ vs $\ell_n(r)$ in Fig. 3. For this case, the volatile regime contributes only 36% of the total mass flow. The viscous regime contributes much more, since most of the surface area is in the smallest pores.

VII. Conclusions

We have constructed a model for mass transport in a porous medium under laser irradiation. We have considered the two limiting cases for the flow of vapor from the pores. In one limit, the flow of vapor from its production site occurs very quickly compared to the rate of pressure buildup due to the highly connected pore structure of the sand model. Inclusion of internal vaporization will then reduce internal temperature excursions by increasing the mass loss. For pore sizes of interest, the temperature suppression may be significant. In the other limit, the pressure builds up in the pores. For a pore tree model, we have shown that the smallest pores act as if they were cut off and only pores in the volatile regime contribute to the mass flow. Hence, while the energy profile will not be affected much in the material, material damage, i.e., mass removal, may result from the high internal pressures. This material damage could be used as an experimental measure to distinguish between the pore tree and sand model. If the ejected material is collected and its porosity measured, then in the pore tree model we would expect much higher porosity than the initial porosity. Future research should concentrate on more realistic models of the pore structure and attempt to take the details of the temperature distribution into account in obtaining the effective surface area.

Acknowledgments

The authors would like to thank G. Simons for many useful discussions. This work was partially supported by the Free Electron Laser Simulation program sponsored by the Air Force through the U.S. Army Strategic Defense Command, Huntsville, Alabama.

References

[1]Anisimov, S., "Vaporization of Metal Absorbing Laser Radiation," *Soviet Physics* JETP, Vol. 27, 1968, pp. 182–183.

[2]Knight, C., "Evaporization from a Cylindrical Surface into Vacuum," *Journal of Fluid Mechanics,* Vol. 75, 1976, pp. 469–486.

[3]Knight, C., "Theoretical Modeling and Rapid Surface Vaporization with Back Pressure," *AIAA Journal,* Vol. 17, 1979, pp. 519–523.

[4]Brunauer, S., Emmett, P. H., and Teller, E., *Journal of the American Chemical Society,* Vol. 60, 1938, p. 309.

[5]Simons, G. A., "The Pore Tree Structure of Porous Char," *Nineteenth Symposium (International) on Combustion,* 1982, pp. 1067–1076.

[6]Simons, G. A., "The Role of Pore Structure in Coal Pyrolysis and Gasification," *Prog. Energy Combustion Sci.,* Vol. 9, 1983, p. 269.

[7]Simons, G. A., "Coal Pyrolysis II. Species Transport Theory," *Combustion and Flame,* Vol. 55, 1984, pp. 181–194.

[8]Cunningham, R. E. and Williams, R. J. J., *Diffusion in Gases and Porous Media,* Plenum Press, 1980, p. 77.

[9]Jean, J., *The Dynamical Theory of Gases,* Dover, 1984.